Enhancement of Electrical Properties of Anisotropically Conductive Adhesive Joints via Low Temperature Sintering

Yi Li, Kyoung-sik Moon, C. P. Wong

School of Materials Science and Engineering, Georgia Institute of Technology, Atlanta, Georgia 30332-0245

Received 10 April 2005; accepted 23 June 2005
DOI 10.1002/app.22509
Published online in Wiley InterScience (www.interscience.wiley.com).

ABSTRACT: The electrical properties of anisotropically conductive adhesives (ACAs) joints through low temperature sintering of nano silver (Ag) particles were investigated and compared with that of the submicron-sized Ag-filled ACA and lead-free solder joints. The nano Ag particles used exhibited sintering behavior at significantly lower temperatures (<200°C) than at the bulk Ag melting temperature (960°C). The sintered nano Ag particles significantly reduced the joint resistance and enhanced the current carrying capability of ACA joints. The improved electrical performance of ACA was attributed to the reduced interfaces between the Ag particles and the increased interfacial contact area between nano Ag particles and bond pads by the particle sintering. The reduced joint resistance was comparable to that of the lead-free (tin/3.5 silver/0.5 copper) metal solder joints. © 2005 Wiley Periodicals, Inc. J Appl Polym Sci 99: 1665–1673, 2006

Key words: nanocomposite; anisotropically conductive adhesives; sintering; epoxy resins; interfaces

INTRODUCTION

The eutectic tin/lead (Sn/Pb) solder alloy has been a primary interconnect material in most areas of electronic packaging, including various packaging and interconnection technologies such as pin through hole, surface mount technology, ball grid array, chip scale package, flip-chip, etc.[1,2] There are increasing concerns nowadays about the use of tin/lead alloy solders, because lead, a major component in solder, has long been recognized as a health threat to human beings.[3–5] Lead-free metal solders such as tin/silver or tin/silver/copper and electrically conductive adhesive have been recognized as two promising alternatives for the traditional lead-bearing solder alloys.[6,7] Lead-free solders, although exhibit competitive electrical conductivity, have a critical issue of much higher processing temperature than conventional tin/lead eutectic solders, which limits their wide application to some extent. Electrically conductive adhesives, a composite that consists of conducting particles dispersed throughout a polymer matrix to provide both attachment and electrical interconnection between electrodes, can be processed at much lower temperatures.

There are two types of conductive adhesives: anisotropically conductive adhesives/films (ACAs/ACFs) and isotropically conductive adhesives (ICAs). ICAs are electrically conductive along all the directions and the loading level of conductive fillers (mostly Ag) exceeds the percolation threshold, while ACAs/ACFs provide unidirectional electrical conductivity in the vertical or *z*-axis by using a relatively low filler loading of conductive fillers. The loading level of ACA is far below the percolation threshold and the low loading is insufficient for interparticle contact, which prevents conductivity in the *x*–*y* plane of the adhesives. The *z*-axis conductive adhesive, in a film or paste form, is interposed (sandwiched) between the two bonding surfaces. Application of heat and pressure to this stack-up interconnection structure causes conductive particles to be trapped between opposing conductor surfaces on the two components (a metal bump of a chip and a bond pad of a substrate). Once electrical continuity is achieved, the dielectric polymer matrix is hardened by chemical reaction (thermosets-cured) or by cooling (thermoplastics-solidified). The hardened dielectric polymer matrix holds the two components together and maintains the pressurized contact between component surfaces and conductive particles. This structure provides the electrical interconnect of these two components. Figure 1 illustrates a cross section of a joint formed by an ACA between the component and the substrate. ACAs/ACFs have been

Correspondence to: C. P. Wong (cp.wong@mse.gatech.edu).
Contract grant sponsor: National Science Foundation; contract grant number: NMI-0217910.
Contract grant sponsor: Environmental Protection Agency; contract grant number: RD-83148901.

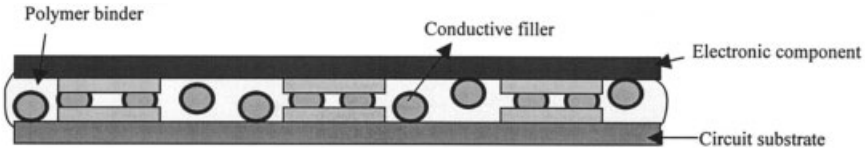

Figure 1 Illustration of a chip and substrate assembled by ACAs incorporated with micronmeter-sized conductive fillers.

widely used for high-density interconnection of liquid-crystal display (LCD) driver chips. Currently, typical ACAs contain the conductive particles with micron meter sizes of 5–10 μm. For the next generation of fine pitch applications, smaller conductive fillers such as nano-sized conductive fillers are expected to be employed in ACAs.

Compared with the traditional soldering technology, ACAs offer numerous advantages such as an easier process, low processing temperatures, lead-free, fluxless bonding that eliminates the need for postassembly cleaning and the disposal of detergent and flux residual, elimination of underfilling process because the ACA resin acts as an underfill that saves process time and cost, and especially, the fine pitch capability which enables the miniaturization of electronic devices.[8–10]

Despite these promising characteristics of ACAs, there are some key issues that hinder their implementation as interconnect materials for high performance devices such as microprocessor and application specific integrated circuit (ASIC) applications. The ACA joints have lower electrical conductivity and poor current carrying capability due to the restricted contact area and poor interfacial bonding of the ACAs and metal bond pads, compared with the metallurgical joint of the metal solders.[9,11,12]

One of the approaches to minimize the joint resistance is to make the conductive fillers fuse each other and form metallic joints such as metal solder joints. However, to fuse metal fillers in polymers does not appear feasible, since a typical organic printed circuit board, on which the metal filled polymer is applied, cannot withstand such a high temperature; the melting temperature (T_m) of Ag, the most commonly used filler, is around 960°C. It has been found that the T_m or the sintering temperatures of materials could be dramatically reduced by decreasing the size of the materials.[13–15] It has been reported that the surface premelting and sintering processes are a primary mechanism of the T_m depression of the fine nano particles.[14] For nano-sized particles, sintering behavior could occur at much lower temperatures; as such, the use of the fine metal particles in ACAs would be promising for fabricating high electrical performance ACA joints through eliminating the interface between metal fillers. The application of nano-sized particles can also increase the number of conductive fillers on each bond pad and result in more contact area between fillers and bond pads. Therefore, application of nano-sized particles has potentials to improve the current density of the ACA joints by distributing current into more conductive paths (Fig. 2).

In this study, ~500- and ~20-nm-sized Ag particles were used as conductive fillers for ACAs. The microstructures and electrical properties were compared. The morphology of the Ag particles after annealing at various temperatures was observed using scanning electron microscopy (SEM). The impacts of nano Ag sintering on the electrical properties of ACAs joints were discussed.

EXPERIMENTAL

Two types of Ag particles, ~500-nm-sized Ag (from Ferro. Corp., South Plainfield, NJ) and ~20-nm-sized

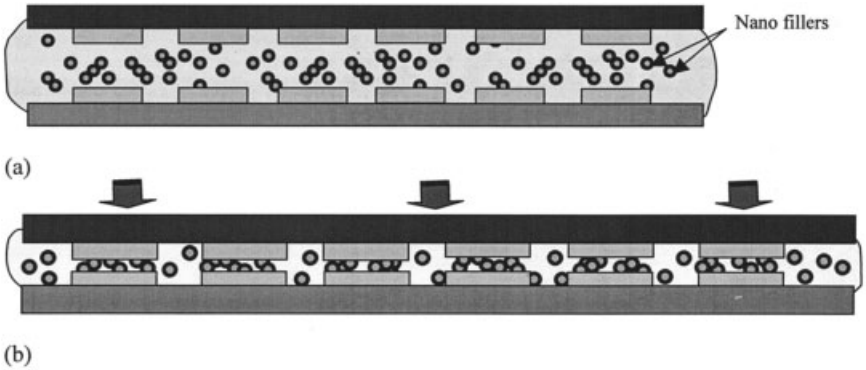

Figure 2 Illustration of a chip and substrate assembled by ACAs incorporated with nanometer-sized conductive fillers; (a) before and (b) after assembly with temperature and pressure applied.

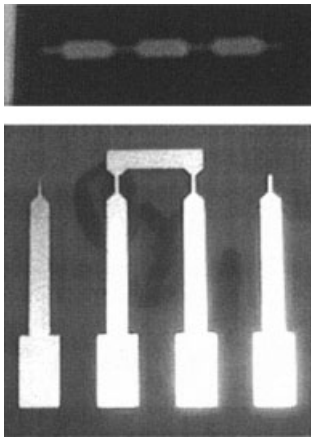

Figure 3 Bond pad surface with gold-finished polyimide for the electrical properties measurement of ACAs.

Ag particles, synthesized by combustion chemical-vapor condensation (CCVC) method using $AgNO_3$ as a precursor,[16] were used. The Ag particles were annealed at different temperatures (from 100 to 250°C). The morphology of the annealed Ag particles was observed by scanning electron microscopy (SEM, Hitach S-800).

To study the effects of curing/sintering behavior of Ag fillers and the electrical performance of ACAs, two different catalysts with low and high curing peak temperatures were used in a typical resin formulation to achieve different temperature curable ACAs. Diglycidyl ether of bisphenol-F (DGEBF) EPON 862 and a methylhexa-hydrophthalic anhydride (HMPA) were used as epoxy and hardener, respectively. 1-cyanoethyl-2-ethyl-4-methylimidazole (2E4MZCN) and cobalt (II) acetylacetonate (Co(II)AcAc) were employed as the catalyst for low temperature and high temperature curable formulations, respectively. The curing profiles of the ACA resins were determined using a modulated differential scanning calorimeter (MDSC) from TA Instruments, model 2970. Dynamic MDSC scans were made on the samples at a heating rate of 5°C/min, from 25 to 350°C. After the dynamic scan, the sample was cooled to room temperature and then rescanned at the same heating rate from 25 to 250°C.

Three to seven volume percent of 20-nm-sized Ag particles were dispersed in the ethylene glycol (EG) solvent and annealed at various temperatures. The EG solution was used for the feasibility study of temper-

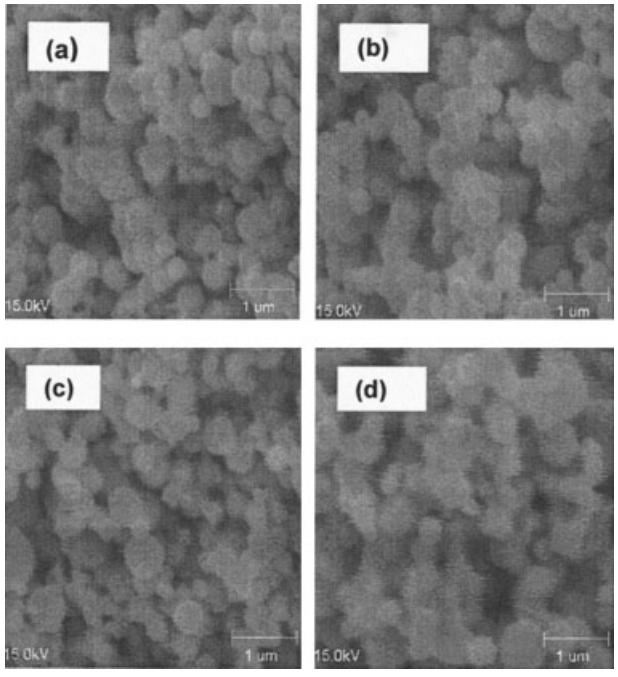

Figure 4 SEM photographs of 500-nm-sized Ag particles annealed at different temperatures for 30 min: (a) room temperature (no annealing); (b) annealed at 100°C; (c) annealed at 150°C; and (d) annealed at 220°C.

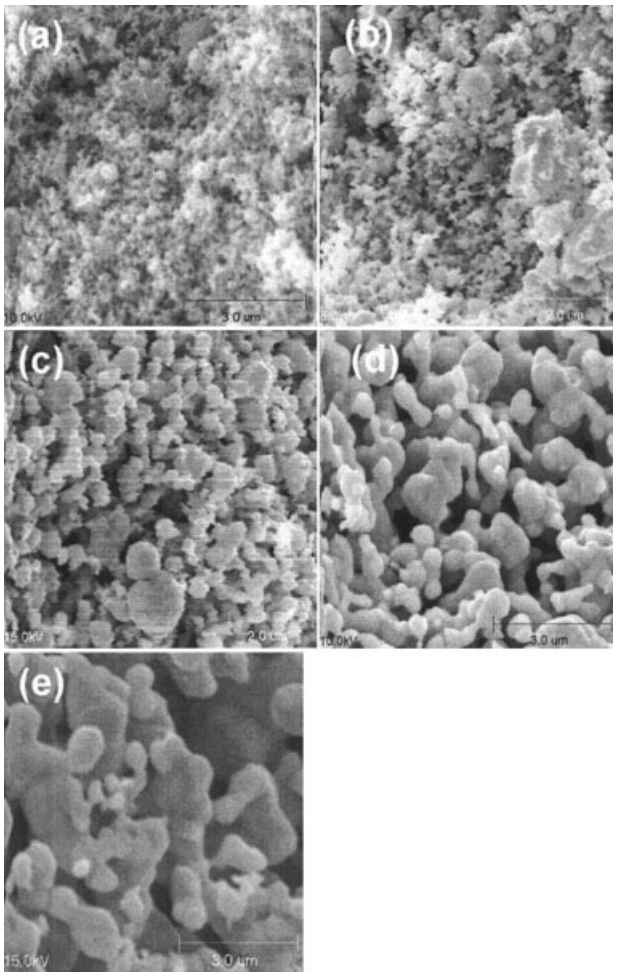

Figure 5 SEM photographs of 20-nm-sized Ag particles annealed at different temperatures for 30 min: (a) room temperature (no annealing); (b) annealed at 100°C; (c) annealed at 150°C; (d) annealed at 200°C; and (e) annealed at 250°C.[13]

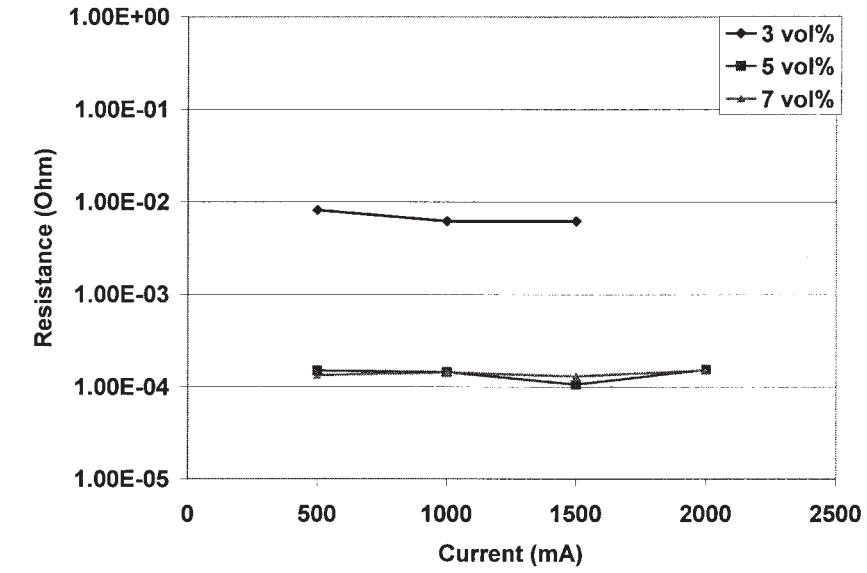

a)

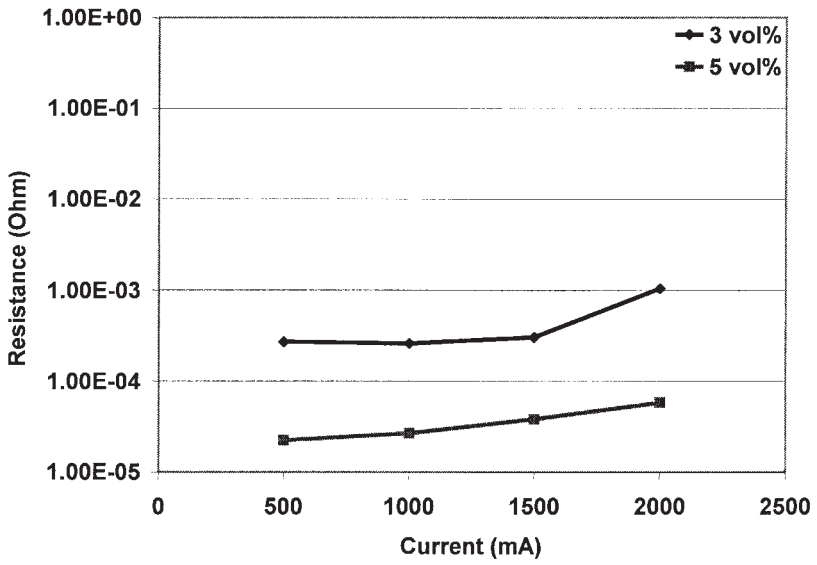

b)

Figure 6 Current–voltage (I-V) relationship of a mixture of 20-nm-sized Ag–ethylene glycol annealed at (a) 150°C for 60 min and (b) 200°C for 30 min.

ature effects of nano Ag on electrical properties. Then 5 vol % of 500- and 20-nm-sized Ag particles were added into ACA resins and cured. The electrical resistance of the contact joints (contact area: 100 × 100 μm^2) of ACAs and lead-free metal solder (tin/3.5 silver/0.5 copper, Indium Corp., Utica, NY) was measured by a four-point probe method. The metal bond pad was a gold-plated polyimide film substrate. The ACA materials were added in between the bottom part and the top part of the test coupon (Fig. 3). Various currents from 500 to 4000 mA were applied by a power supplier (HP model 6553A), and the voltage of the interconnect joints were measured by a Keithley 2000 multimeter (Cleveland, OH).[12]

RESULTS AND DISCUSSION

Sintering of nano Ag particles

To study the sintering behavior of Ag particles, the Ag particles were annealed at different temperatures (100,

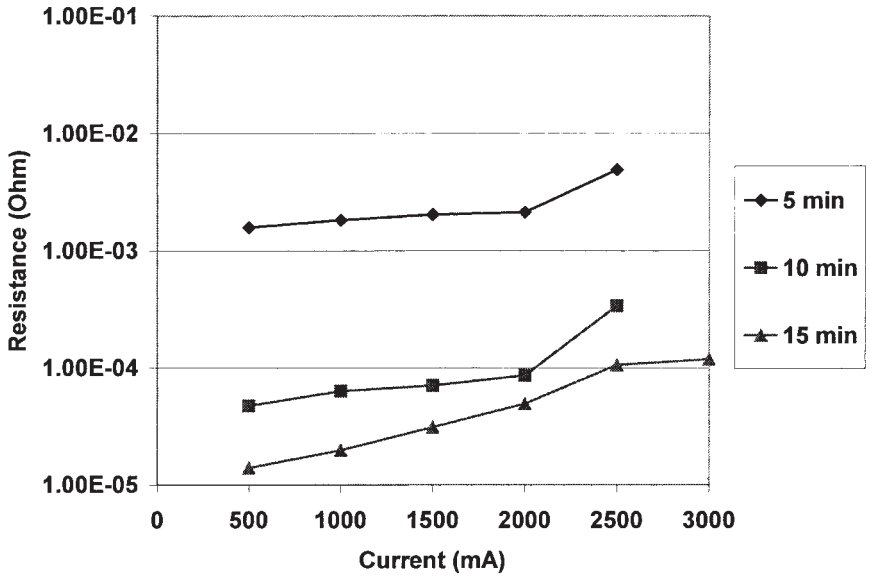

Figure 7 Current–voltage relationship of 5 vol % nano Ag particles in an epoxy resin annealed at 200°C for different time.

150, 200, and 250°C). From SEM photographs, the 500-nm-sized Ag particles showed no significant change in morphology and particle size after annealing; no significant sintering behavior was observed (Fig. 4). However, 20-nm-sized particles exhibited a markedly different morphology, as shown in Figure 5. Obvious sintered nano particles were observed at 150°C and higher temperatures.[13] Particles annealed at 150°C and higher temperatures were fused through their surface and many of dumbbell type particles could be found. The morphology was similar to a typical morphology of an initial stage in the typical sintering process of ceramic, metal, and polymer powders. This low temperature sintering behavior of the nano particles is attributed to the extremely high interdiffusivity of the nano particle surface atoms, because of the significantly energetically unstable surface status of the nano particles, in particular, their high surface-to-volume ratios.

Electrical performance of sintered nano Ag particles in ethylene glycol

The nano particle sintering behavior may help improve the interfaces between sintered particles as well as the conductive adhesives/metal bond pads of the substrate and the components. For the sintering reaction in a certain material system, annealing temperature and holding time are the most important parameters, since sintering is a temperature- and time-dependent process.

To study the effect of annealing temperature on the nano Ag sintering and the joint resistance of metal fillers and metal bond pads, the nano Ag particles were dispersed into the ethylene glycol solvent (EG) and annealed at 150 and 200°C for 60 and 30 min, respectively. To mimic the typical ACA processing, pressure ($\sim$100 g/cm^2) was applied to the joint during the annealing process. The joint resistance of nano Ag with bond pad was recorded and shown in Figure 6. With increasing the concentration of nano Ag fillers in ethylene glycol, the obviously lower joint resistance was achieved. For annealing at 150°C, the joint resistance was 10^{-2} Ohm for 3 vol % of 20-nm-sized Ag in EG, and the highest current applied without inducing joint failure (endurable current) was 1500 mA. Increasing the nano Ag concentration to 5 and 7 vol % led to a significantly reduced joint resistance of 10^{-4} Ohm and a higher endurable current of 2000 mA. When the temperature was raised to 200°C, the joint resistance was further decreased. The joint resistance of 3 and 5 vol % 20-nm-sized Ag particles annealed at 220°C was around 5×10^{-4} and 5×10^{-5} Ohm, respectively, while the resistance of 7 vol % 20-nm-sized Ag was too low to be measured. The improved joint resistance with higher temperature treatment was considered to be due to the further sintering of nano Ag particles. The joint resistance (R) is the sum of Ag filler resistance (R_{Ag}) and interparticle resistance (R_{int}) along the z direction. The sintered structure reduced the number of interparticle interfaces, therefore, the total interparticle resistance was decreased. The resistance of fillers depends on the intrinsic properties of the fillers and is much lower compared with the contact resistance between fillers. Thus, the joint resistance was mostly determined by the interparticle resistance. Therefore, the sintering of nano Ag particles and consequently the decreased interparticle resistance contributed to the significantly reduced joint resistance.

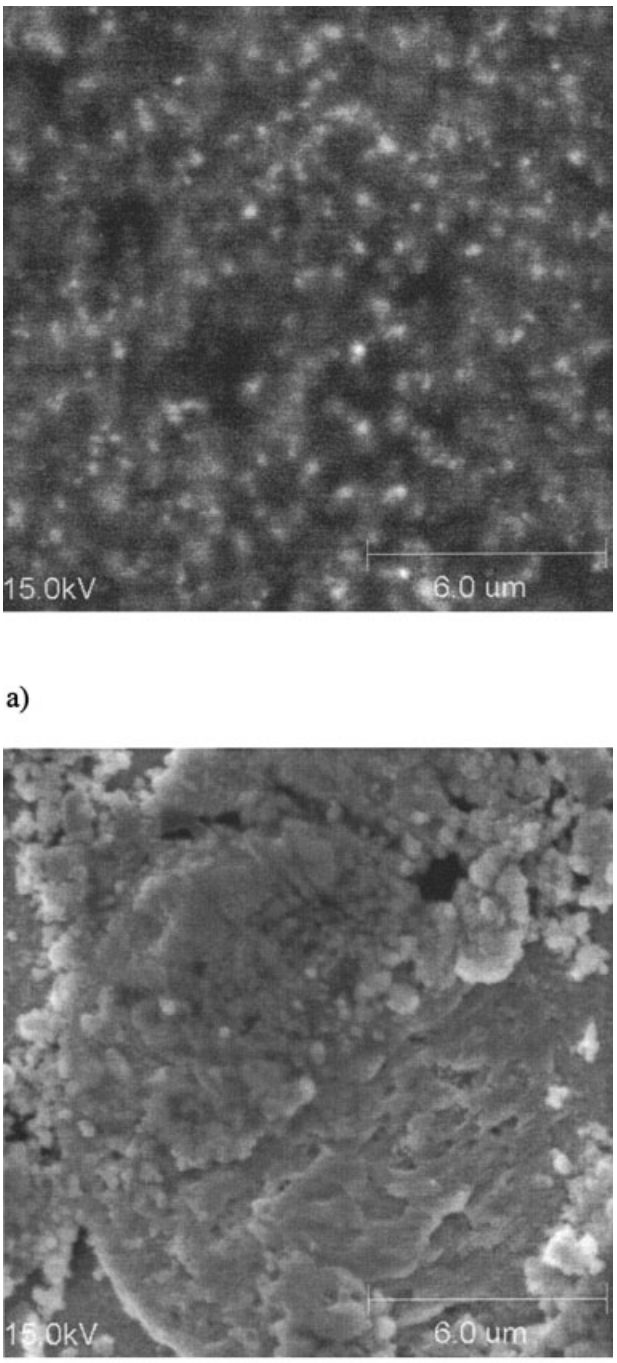

Figure 8 SEM pictures of the peeled conduction joints after annealing at 200°C for: (a) 5 min and (b) 30 min.

Effects of annealing time on the sintering and electrical performance of nano ag filled adhesive joint

Effect of annealing time on the sintering and the electrical performance of nano Ag filled adhesive joints was also studied. Five volume percent of 20-nm-sized Ag fillers were dispersed in the resin. To prevent the crosslinking reaction of the resin, no catalyst was used. The adhesives with 5 vol % 20-nm-sized Ag fillers were annealed at 200°C for various times. As can be seen from Figure 7, after 5 min annealing, the joint resistance was 10^{-3} to 10^{-2} Ohm and the current carrying capability was 2500 mA. After annealing for 10 min, significantly lower joint resistance was achieved and the current carrying capability was the same as 5-min-treated samples (2500 mA). With increasing current from 500 to 2500 mA, the joint resistance increased from 5×10^{-5} to 5×10^{-4} Ohm. When the annealing time increased to 15 min, even lower joint resistance of 10^{-5} Ohm was obtained. Furthermore, the highest endurable current also increased to 3000 mA. The dramatically lower joint resistance and higher current carrying capability with longer annealing time may be attributed to the further sintering of nano Ag fillers. The further sintering of nano Ag particles enabled the reduction of interparticle interfaces. Subsequently, it could be easier for the electrons to transport between Ag fillers. Therefore, lower interparticle resistance and joint resistance were achieved. The SEM pictures of the top view of the joints obtained by peeling off the top electrode after annealing at 200°C for different time are shown in Figure 8. After

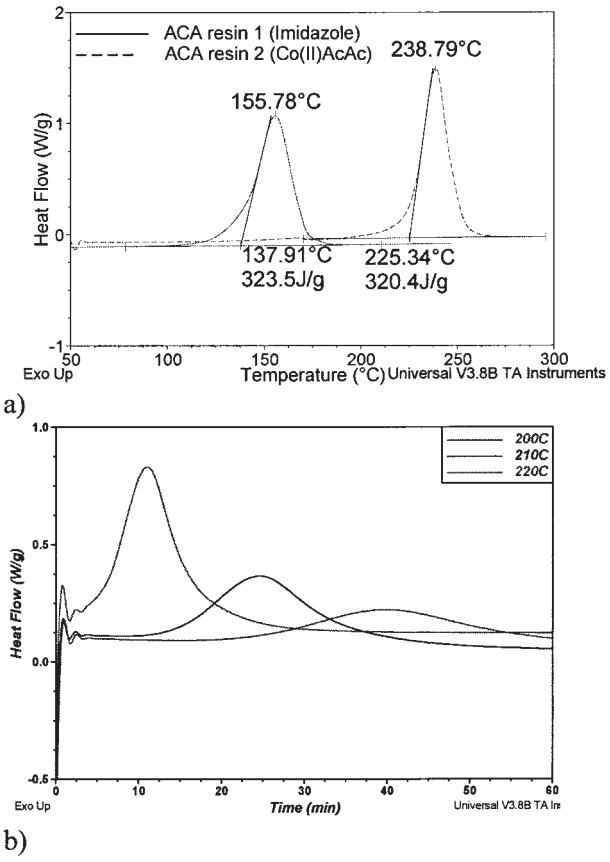

Figure 9 Curing profile of ACA resins: (a) dynamic DSC for resins with different catalysts; (b) isothermal DSC for resin with high curing latency.

TABLE I
Curing Profiles of ACA Resins with High Curing Latency

Isothermal temperature (°C)	Reaction time (min)	Total reaction heat (J/g)
200	60	169.3
210	45	254.7
220	30	324.6

being annealed at 200°C for 5 min, the nano particles were dispersed well in the epoxy resin and no obvious sintering behavior was observed. When the samples were annealed for 30 min, sintered particles were observed in the epoxy resin.

Effects of particle size and nano Ag sintering on the electrical properties of ACA

To study the sintering behavior of nano Ag particles in the ACA formulations, two resin systems with two

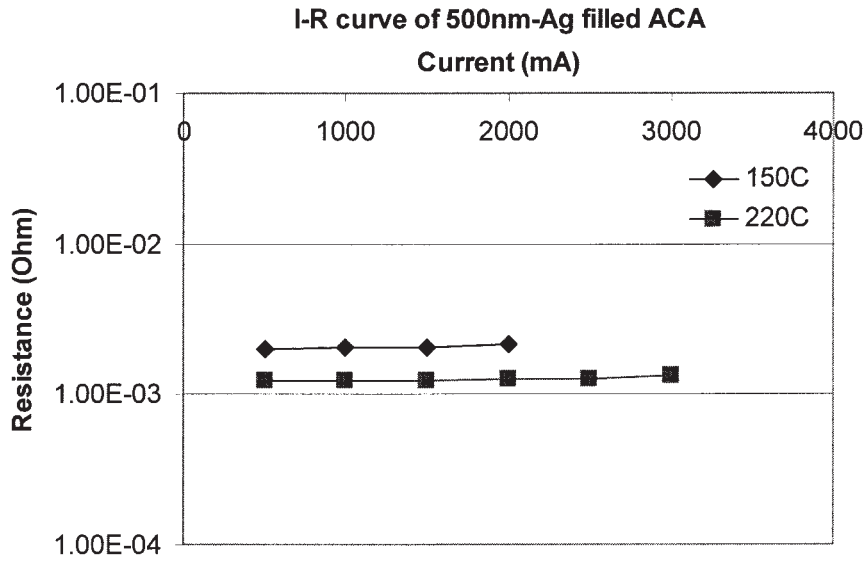

a)

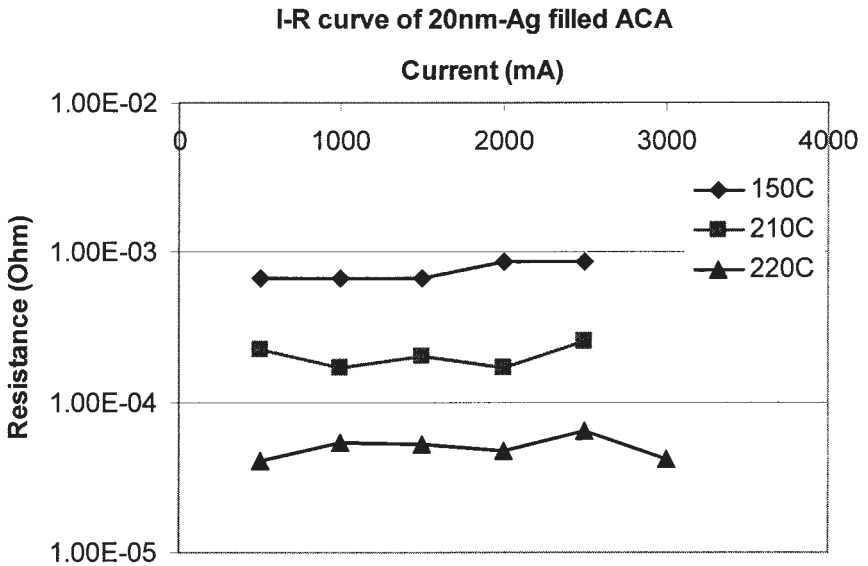

b)

Figure 10 Current–voltage relationship of ACAs with different curing conditions: (a) 500-nm Ag filled ACA; (b) nano-sized Ag filled ACA.

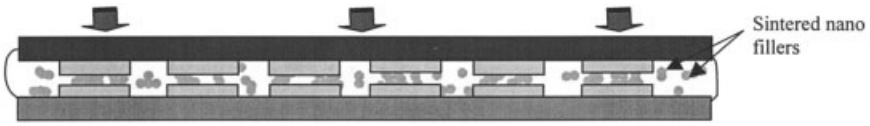

Figure 11 Schematic illustration of ACA joint with sintered nano Ag fillers.

different curing temperatures were selected. 2E4MZCN and Co(II)AcAc were used as catalysts for low and high curing temperatures, respectively. The curing profiles of the resins are shown in Figure 9. The resin 1 with 2E4MZCN had a curing peak at 156°C, while resin 2 with Co (II)AcAc started curing at 190°C and the curing peak occurred at 239°C, at a scan rate of 5°C/min. For resin 2, isothermal DSC was run at three different curing temperatures, 200, 210, and 220°C for 60 min each. The isothermal reaction heats of the resin cured at different temperatures are shown in Table I. With increasing temperatures, the total reaction heats increased because of the higher degree of curing. Compared with the reaction heat from dynamic DSC result, 210°C is required for the curing of resin 2. Therefore, 150 (resin 1), 210, and 220°C (resin 2) were used and cured for 60, 45, and 30 min, respectively.

The current-voltage relationship of the 500- and 20-nm-sized Ag filled ACAs is shown in Figure 10. As can be seen from these figures, with increasing curing temperatures, the resistance of the ACA joints decreased and the current carrying capability increased. For 20-nm-sized Ag filled ACAs, the joint resistance decreased dramatically from 7×10^{-4} to 5×10^{-5} Ohm when increasing the processing temperature from 150 to 220°C by using different catalysts. Also, the ACAs with higher curing temperature exhibited higher current carrying capability of 3000 mA than the low temperature curable samples (2500 mA). This phenomenon suggested that further sintering of nano Ag particles at higher temperature contributed to the superior electrical properties at the interface between fillers and metal bond pads. From the illustration shown in Figure 11, after the nano Ag-filled ACAs were cured under the application of pressure, there was good contact between Ag fillers and metal bond pad, and a high electrical conduction was achieved. For typical ACAs, the physical contact between fillers and bond pad gave a relatively higher joint resistance. With the sintering behavior, the nano Ag particles in the ACA formulations could fuse each other through their surfaces, which decreased the number of interfaces between particles. Therefore, the significantly improved joint resistance and current carrying capability were achieved at higher temperatures. For the 500-nm-sized Ag filled ACA, moderate improvement of joint resistance with higher processing temperature was observed from 2×10^{-3} to 1×10^{-3} Ohm, and the current carrying capability was also increased to 3000 mA. The improvement was not as significant as that of nano Ag filled ACA, because of the lack of sintering behavior of conductive fillers.

The electrical properties of lead-free solder joints, conventional ACAs, nano Ag filled ACAs (processed below sintering temperature), and sintered nano Ag ACAs were measured and compared in Figure 12. For

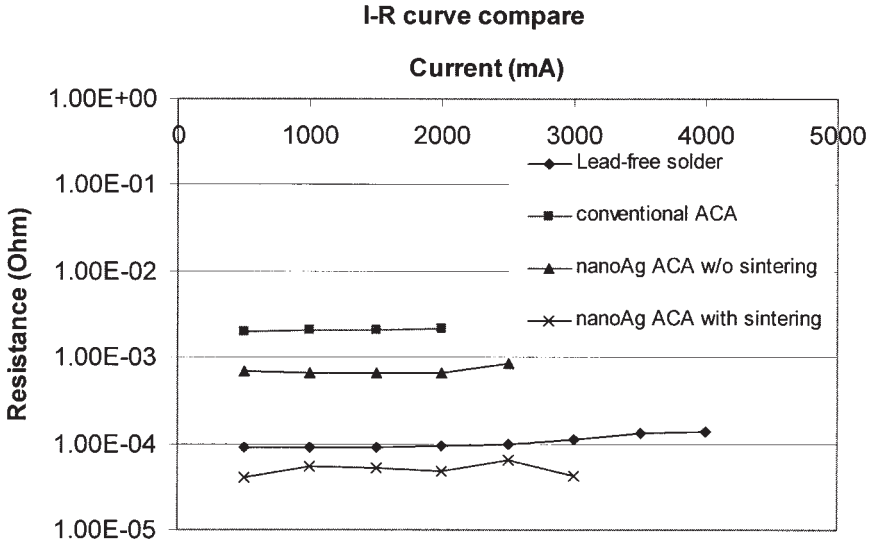

Figure 12 Comparison of current–voltage relationship of lead-free solders (tin/3.5 silver/0.5 copper), conventional ACA, nano-Ag ACA without sintering and nano-Ag ACA with sintering.

the lead-free solder joints, the resistance was 10^{-4} Ohm and the current carrying capability was 4000 mA. In spite of many advantages of ACA,[8–10] conventional ACAs had much higher joint resistance and lower current carrying capability than the metal solder joints. The joint resistance of the conventional was 2×10^{-3} Ohm and current carrying capability was only 2000 mA. By using the nano Ag fillers, the resistance was improved to 7×10^{-4} Ohm and current carrying capability was increased to 2500 mA. Furthermore, when nano Ag particles were sintered in the ACA resins, the joint resistance was achieved as 5×10^{-5} Ohm, which was even lower than that of the solder joints. At the same time, the current carrying capability was also further improved to 3000 mA.

CONCLUSIONS

Although the Ag particles have a high melting point of 960°C, obvious sintering behavior was observed for nano Ag particles at much lower temperatures (<200°C). The sintering of nano Ag particles in anisotropically conductive adhesives (ACA) reduced the joint resistance and enhanced current carrying capability significantly. The enhanced electrical properties of the ACA joints were attributed to the reduced number of particle interfaces and improved interfacial contact between nano Ag fillers and bond pads by sintering and compressing processes of the ACA. The reduced joint resistance was comparable to or even better than that of the lead-free metal joints.

References

1. Lau, J.; Wong, C. P.; Lee, N. C.; Lee, S. W. R. Electronics Manufacturing: With Lead-Free, Halogen-Free, and Conductive-Adhesive Materials; McGraw Hill: New York, 2002.
2. Puttlitz, K. J.; Kathleen, A. S., Eds. Handbook of Lead-free Solder Technology for Microelectronic Assemblies; Marcel Dekker: New York, 2004; Chapter 1.
3. Abet, M.; Selvaduray, G. Mater Sci Eng 2000, 27, 95.
4. Trumble, B. IEEE Spectrum, May 1998, 55.
5. Gilleo, K. Circuits Assembly January 1994, 52; February 1994, 50.
6. Li, Y.; Moon, K.; Wong, C. P. Science 2005, 308, 1419.
7. Small, D. J.; Eisenach, B.; Lewis, A.; Babiarz, A. Advanced Packaging January 1999, 38.
8. Nguyen, G.; Williams, J.; Gibson, F. ISHM Proceedings 1992, 510.
9. Li, Y.; Wong, C. P. In IEEE Proceedings Polytronic 2004: 4th International IEEE Conference on Polymers and Adhesives in Microelectronics and Photonics; Portland, OR, September 14–16 2004; p 1.
10. Jagt, J. C.; Beric, P. J. M.; Lijten, G. F. C. M. IEEE Trans Compon Packag Manuf Technol B 1995, 18, 292.
11. Liu, J., Ed. Conductive adhesives for Electronics Packaging; Electrochemical Publications: British Isles, 1999.
12. Li, Y.; Moon, K.; Wong, C. P. J Electron Mater 2005, 34, 266.
13. Moon, K.; Dong, H.; Maric, R.; Pothukuchi, S.; Hunt, A.; Li, Y.; Wong, C. P. J Electron Mater 2005, 34, 132.
14. Matsuba, Y. Erekutoronikusu Jisso Gakkaishi 2003, 6, 130.
15. Efremov, M. Y.; Schiettekatte, F.; Zhang, M.; Olson, E. A.; Kwan, A. T.; Berry, R. S.; Allen, L. H. Phys Rev Lett 2000, 85, 3560.
16. Hunt, A. T.; Carter, W. B.; Cochran, J. K. Appl Phys Lett 1993, 63, 266.